

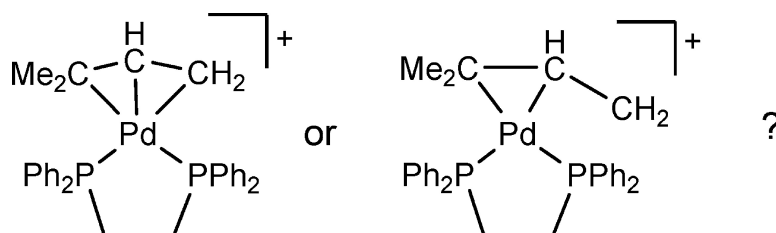
Article

Is the Allylpalladium Structure Altered between Solid and Solutions?

Eric Clot, Odile Eisenstein, Tsu-Chien Weng, James Penner-Hahn, and Kenneth G. Caulton

J. Am. Chem. Soc., **2004**, 126 (29), 9079-9084 • DOI: 10.1021/ja049091g • Publication Date (Web): 02 July 2004

Downloaded from <http://pubs.acs.org> on March 31, 2009



More About This Article

Additional resources and features associated with this article are available within the HTML version:

- Supporting Information
- Access to high resolution figures
- Links to articles and content related to this article
- Copyright permission to reproduce figures and/or text from this article

[View the Full Text HTML](#)



Is the Allylpalladium Structure Altered between Solid and Solutions?

Eric Clot,[†] Odile Eisenstein,[†] Tsu-Chien Weng,[‡] James Penner-Hahn,[‡] and Kenneth G. Caulton^{*,§}

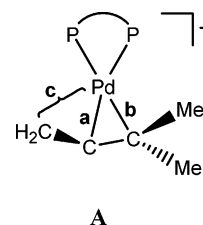
Contribution from the LSDSMS (UMR 5636), case courrier 14, Université Montpellier 2, 34095 Montpellier Cedex 5, France, The University of Michigan, 930 North University Avenue, Ann Arbor, Michigan, 48109, and Department of Chemistry, Indiana University, 800 East Kirkwood Avenue, Bloomington, Indiana 47405

Received February 18, 2004; E-mail: caulton@indiana.edu

Abstract: Recent EXAFS measurements on $[(\text{Ph}_2\text{PCH}_2\text{CH}_2\text{PPh}_2)\text{Pd}(\text{H}_2\text{CCHCMe}_2)]\text{O}_3\text{SCF}_3$ (Tromp et al. *J. Am. Chem. Soc.* **2002**, *124*, 14814) were interpreted as evidence that, when the complex is dissolved in THF, the allyl ligand adopts an η^2 structure with a dangling allyl CH_2 substituent. DFT calculations of the Pd complex using $\text{H}_2\text{P}-\text{CH}_2\text{CH}_2-\text{PPh}_2$ as a model for $\text{Ph}_2\text{P}-\text{CH}_2\text{CH}_2-\text{PPh}_2$ (dppe), in the absence or the presence of the triflate counteranion, and modeling the THF solvent by explicit Me_2O molecules or by a continuum model give always a conventional η^3 - $\text{H}_2\text{CCHCMe}_2$ structure with equal Pd–C bonds to the terminal carbon centers of the allyl. QM/MM calculations using the dppe ligand also fail to support an η^2 -allyl structure as a global minimum. The EXAFS parameter space is shown to have multiple minima. These have very similar overall EXAFS, but have very different structural parameters. The minimum that was the basis for the previous structural conclusion gives a slightly better fit but has unrealistic Debye–Waller factors and threshold energies.

Introduction

It has recently been proposed¹ that the cation $(\text{dppe})\text{Pd}[\text{H}_2\text{CCH}(\text{H})\text{CMe}_2]^+$ has different structures in the solid state and in THF solution (dppe is $\text{Ph}_2\text{P}(\text{CH}_2)_2\text{PPh}_2$, and the counterion is F_3CSO_3^-). The solution-phase evidence comes from Pd K-edge EXAFS, in the form of small changes in the fitted EXAFS parameters. On going from the solid state to solution, there is a decrease, by one, in the modeled number of Pd–C bonding distances ($N_{\text{C}}^{\text{(allyl)}}$) at 2.2 Å and an increase, by one, in the modeled number of Pd–C nonbonding distances ($N_{\text{C}}^{\text{(nb)}}$) at 3.0 Å. These observations led to the conclusion that the allyl binding is altered from η^3 to η^2 on going from solid to solution. Since the crystal structure shows conventional η^3 -allyl binding and since solid-state EXAFS measurements are in relatively good agreement with the crystal structure (albeit with a Pd–C_{allyl} distance that is 0.07 Å longer than in the crystal), the changes observed in the solution EXAFS were interpreted in terms of a conversion to structure **A** where **a** and **b** are conventional bonding distances (2.15 Å) but **c** is 2.95 Å, a long distance equal to the separation between Pd and one of the methyl carbons. This structural change in solution was suggested to play a role in controlling the regioselectivity of nucleophilic addition to the allyl carbons, as addressed computationally.^{2,3}



These results are remarkable and unprecedented. The idea of a major change in structure on change of phase (where “major” means bond rupture, not merely angular distortion) is often considered, but rarely verified. When a major structural change does occur,^{4–10} it can generally be attributed to (a) weak bonds and (b) compensating bond formation (e.g., bridge/terminal carbonyl conversion in an $\text{M}_2(\text{CO})_2$ unit). In the present case, it is remarkable that one carbon, not two (see below), becomes nonbonding to Pd and that the more distant carbon is *not* the sterically encumbered CMe_2 group, but rather CH_2 (see **A**). The implication of the long distance **c** above is that there should be a carbon-centered radical, as well as a Pd^{I} radical;¹¹

[†] Université Montpellier.

[‡] The University of Michigan.

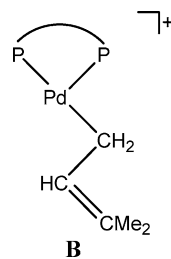
[§] Indiana University.

(1) Tromp, M.; van Bokhoven, J. A.; van Haaren, R. J.; van Strijdonck, G. P. F.; van der Eerden, A. M. J.; van Leeuwen, P. W. N. M.; Koningsberger, D. C. *J. Am. Chem. Soc.* **2002**, *124*, 14814.
(2) Szabó, K. *J. Am. Chem. Soc.* **1996**, *118*, 7818.

(3) Delbecq, F.; Lapouge, C. *Organometallics* **2000**, *19*, 2716.
(4) Zamaraev, K. *New J. Chem.* **1994**, *18*, 13.
(5) Cotton, F. A. *Inorg. Chem.* **2002**, *41*, 643.
(6) Cotton, F. A. *J. Organomet. Chem.* **1975**, *100*, 29.
(7) Bennett, M. A.; Neumann, H.; Willis, A. C.; Ballantini, V.; Pertici, P.; Mann, B. E. *Organometallics* **1997**, *16*, 2868.
(8) Hosang, A.; Englert, U.; Lorenz, A.; Ruppli, U.; Salzer, A. *J. Organomet. Chem.* **1999**, *583*, 47.
(9) Slugovc, C.; Padilla-Martinez, I.; Sirol, S.; Carmona, E. *Coord. Chem. Rev.* **2001**, *213*, 129.
(10) Paneque, M.; Sirol, S.; Trujillo, M.; Carmona, E.; Gutiérrez-Puebla, E.; Monge, M. A.; Ruiz, C.; Malbos, F.; Serra-Le Berre, C.; Kalck, P.; Etienne, M.; Daran, J. C. *Chem. Eur. J.* **2001**, *7*, 3868.

however, the *ordinary* character of the reported solution NMR spectra¹² is inconsistent with such a structure.

Surprisingly, the interpretation of the EXAFS data provides no support for the *traditional* focus of alternative bonding of an allyl ligand, the conversion to an η^1 binding mode (**B**).



An accompanying EXAFS study¹ of $(\text{O}[(2\text{-PPh}_2)\text{C}_6\text{H}_4]_2)\text{-Pd}[\text{CH}_2\text{CHCMe}_2]^+$ showed *no* structural change on going from the solid state to THF solution, although this larger chelate (bite angle of this “DPEphos” is 18° larger than that of dppe) should be more likely to produce the new bonding form of the allyl ligand on Pd. In addition, this lack of structural change for the complex of a related ligand would argue that neither THF coordination to Pd nor nucleophilic attack by triflate is involved in either of the complexes studied (*vide infra*).

Results

Geometry Optimization Using Density Functional Theory.

The data in ref 1 make use of new developments in EXAFS data analysis¹³ and, thus, should be less sensitive to the artifacts¹⁴ that have, on occasion, prevented accurate structure determination by EXAFS. Nevertheless, the fact that EXAFS analyses can give false minima^{15,16} coupled with the unprecedented nature of structure **A** suggests that use of other techniques for structural determination is warranted. If the proposed structural change is a phenomenon which is suppressed by intermolecular forces in the solid state but appears only in a less dense medium (i.e., solution), then this might be a case where the gas-phase (i.e., unimolecular) conditions of DFT calculations could be used advantageously. Thus, we need to better understand both the intrinsic structural preference of the isolated cation and whether this structure can be altered by interactions with the solvent or the counteranion. We therefore undertook a DFT geometry optimization study of this cation to find its intrinsic geometric preference as well as to perhaps find some crude estimate of the energy required to reach geometry **A**, if that could be found as a stationary point on the energy surface.

First, to test the accuracy of our methodology, we optimized the η^3 -allyl structure, **1**, for the model $(\text{dhpe})\text{Pd}(\text{H}_2\text{CCHCMe}_2)^+$ ($\text{dhpe} = \text{H}_2\text{PCH}_2\text{CH}_2\text{PPh}_2$) at the B3PW91 level. The geometry

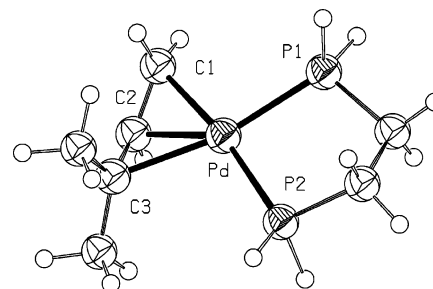


Figure 1. Optimized geometry (B3PW91) for the η^3 -allyl model complex $(\text{dhpe})\text{Pd}(\text{H}_2\text{CCHCMe}_2)^+$ **1**.

Table 1. Comparison of Selected Geometrical Parameters (Distances in Å, Angles in deg) between the X-ray Structure¹² for $(\text{dppe})\text{Pd}(\text{H}_2\text{CCHCMe}_2)^+$ and the Calculated Structures **1** (B3PW91), **1'** (B3PW91/UFF), and **2** (B3PW91 within CPCM, To Model the Effect of Solvent)^a

	exp	1	1'	2
Pd–C1	2.184	2.159	2.186	2.158
Pd–C2	2.174	2.169	2.160	2.162
Pd–C3	2.253	2.295	2.273	2.259
Pd–P1	2.296	2.328	2.348	2.322
Pd–P2	2.293	2.341	2.335	2.328
C1–C2	1.421	1.414	1.411	1.413
C2–C3	1.407	1.414	1.416	1.416
P1–Pd–P2	85.8	85.4	78.8	85.6
C1–C2–C3	121.1	122.6	122.7	122.2
C1–Pd–C3	67.4	67.6	67.6	68.2

^a The numbering of the atoms is shown in Figure 1.

is in good agreement with even subtle features of the experimental data¹² (Figure 1, Table 1).

An ONIOM(B3PW91/UFF) calculation on $(\text{dppe})\text{Pd}(\text{H}_2\text{CCHCMe}_2)^+$, **1'** ($\text{dppe} = \text{Ph}_2\text{PCH}_2\text{CH}_2\text{PPh}_2$), yielded the same geometry (Table 1), thus ruling out a potential elongation of Pd–C1 by the steric bulk of phenyl rings. Our initial search for a structure of type **A** started from a geometry with the allyl CH_2 group 3 Å from Pd (as the solution EXAFS suggested). The resulting optimized geometry was the η^3 -allyl structure **1**, so a pendant CH_2 group within the cation $(\text{dhpe})\text{Pd}(\text{H}_2\text{CCHCMe}_2)^+$ is not an energy minimum supported by DFT calculations in the gas phase. The distorted geometry with the CH_2 group 3 Å from Pd was also a starting geometry for an ONIOM calculation to test whether the Ph groups could make the η^2 -allyl an energy minimum. However, the η^3 -allyl geometry **1'** was again obtained, thus indicating that any elongation of Pd–C1 does not result from modeling the steric influence of the phenyl groups. We therefore sought to simulate solvent effects and performed a DFT optimization within a continuum model (CPCM),¹⁷ starting from the distorted geometry described above. Again, an η^3 -allyl geometry, **2**, was obtained and was in good agreement with the experimental solid-state structural data (Table 1). This model of the influence of solvent, thus, makes no significant change in the structure.

Bond elongation uncompensated by bond formation without an entropy benefit is generally an endothermic process. We therefore investigated processes where an additional bond was formed. The anomalously long bond **c** in **A** could originate from weak interactions of the dangling CH_2 group with *specific* donor solvent molecules. We modeled such a situation (i.e., THF

(11) The alternative is a pendant carbonium, unreactive toward the necessarily *zero-valent* Pd neighbor.

(12) van Haaren, R. J.; Goubitz, K.; Fraanje, J.; van Strijdonck, G. P. F.; Oevering, H.; Coussens, B.; Reek, J. N. H.; Kamer, P. C. J.; van Leeuwen, P. W. N. M. *Inorg. Chem.* **2001**, *40*, 3363.

(13) Tromp, M.; van Bokhoven, J. A.; Arink, A. M.; Bitter, J. H.; van Koten, G.; Koningsberger, D. C. *Chem. Eur. J.* **2002**, *8*, 5667.

(14) One possible artifact is radiation damage. There is no evidence for radiation damage in the present case, and our analysis does not rest on radiation damage as the source of the structural conclusions from solution EXAFS data.

(15) Michalowicz, A.; Vlais, G. *J. Synchrotron Radiat.* **1998**, *5*, 1317.

(16) Clark-Baldwin, K.; Tierney, D. L.; Govindaswamy, N.; Gruff, E. S.; Kim, C.; Berg, J.; Koch, S. A.; Penner-Hahn, J. E. *J. Am. Chem. Soc.* **1998**, *120*, 8401.

(17) Tomasi, J.; Cammi, R.; Mennucci, B.; Cappelli, C.; Corni, S. *Phys. Chem. Chem. Phys.* **2002**, *4*, 5697.

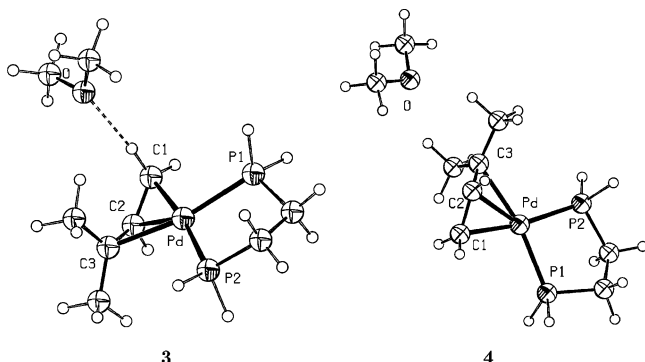
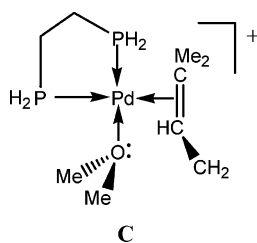


Figure 2. Optimized geometries (B3PW91) for the monocationic Me₂O adducts to the η^3 -allyl complex with C–H \cdots O interactions with C1 (respectively C3), **3** (OMe₂ near CH₂; respectively **4**, OMe₂ near CMe₂).

solvent) by adding an Me₂O molecule within close (2.5 Å) contact to a dangling CH₂ (respectively a dangling CMe₂) group. Only an η^3 -allyl structure, **3** (respectively **4**), was obtained (Figure 2) in which the ether lone pairs form weak C–H \cdots O interactions (O \cdots H = 2.24 Å, **3**; O \cdots H = 2.38 and 2.46 Å, **4**). **3** is slightly more stable than **4** (by 0.8 kcal mol⁻¹), and the binding energy of Me₂O in the hydrogen bond of **3**, 6.5 kcal mol⁻¹, is not large enough to compensate for the unfavorable entropy change of the process ($T\Delta S^\circ = 8$ –10 kcal mol⁻¹ at 298 K).¹⁸ The geometry optimization therefore suggests that this (oxonium) O–C (allyl) bond is weaker than a Pd–C(allyl) bond and essentially free Me₂O. Thus, ether binding to the CH₂ cannot thermodynamically drive formation of structure **A**. A chemically plausible alternative, with Me₂O bound to Pd and an η^1 -allyl, had a minimum that was either 14.2 kcal mol⁻¹ (CH₂ bound to Pd, **5**) or 24.6 kcal mol⁻¹ (CMe₂ bound to Pd, **6**) higher than that for **3**, respectively (Figure 3). This is in qualitative agreement with calculations by Szabó and Solin on the mechanism of $\eta^3 \leftrightarrow \eta^1$ isomerization in allylpalladium complexes.¹⁹

Note that an attempt to optimize an η^1 -allyl geometry (i.e., **B**) on (dhpe)Pd(H₂CCHCMe₂)⁺ failed and always gave the η^3 -allyl. A geometry optimization beginning from **C** (CH₂ \cdots Pd = 3 Å, O \cdots CH₂ = 2.41 Å) was studied to evaluate possible stabilization of the dangling CH₂ by interaction with one lone pair of a coordinated Me₂O. This starting geometry optimized



to an η^3 -allyl adduct, with the Me₂O dissociated from Pd and interacting weakly with one H of the resulting complex as in **3** and **4**.²⁰

(18) Watson, L. A.; Eisenstein, O. *J. Chem. Educ.* **2001**, *79*, 1269.

(19) Solin, N.; Szabó, K. *Organometallics* **2001**, *20*, 5464.

(20) We have shown with ONIOM calculations on **1'** that the phenyl groups do not perturb the first coordination sphere around Pd drastically. Therefore, there should not be any particular influence of Ph groups on the second coordination sphere associated with external interaction between the allyl ligand and the solvent or the counteranion. Consequently, we did not perform any ONIOM calculations on systems such as **3** and **4** with dhpe replaced by dppe.

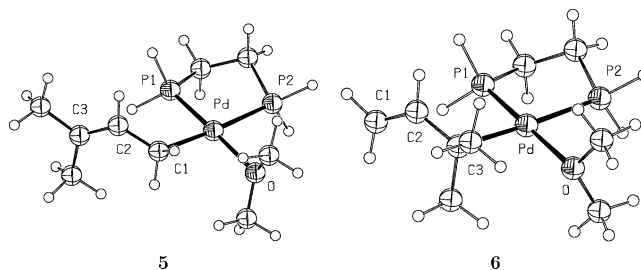
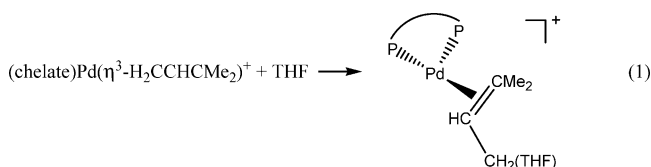


Figure 3. Optimized geometries (B3PW91) for the monocationic η^1 -allyl complexes **5** and **6** with Me₂O coordinated to Pd and either CH₂ (**5**) or CMe₂ (**6**) coordinated to Pd.

We also considered an alternative structural rearrangement, this one induced by THF (eq 1, THF modeled by Me₂O in the calculations). This involves nucleophilic attack on the less bulky allyl carbon to make an oxonium ion pendant to an olefin on Pd(0). Geometry optimization beginning with a C–O distance



of 1.56 Å, a typical single bond, led to dissociation of this bond and formation of an η^3 -allyl structure (not shown), similar to **3**. We also searched for nucleophilic attack on the allyl carbon atoms by triflate as a stronger nucleophile than THF. To take into account the solvation energy of the charged species with respect to the neutral systems, geometry optimizations have been carried out at the B3PW91 level within a continuum solvation model (CPCM). Attack at C1 (respectively C3) yielded the Pd(0) olefin complex **7** (respectively **8**) with a long Pd–C1 distance of 3.006 Å (respectively Pd–C3 = 3.110 Å, see Figure 4). Complex **7** has a structure that could potentially correspond to the target geometry **A** and could be at the origin of the EXAFS observation if its energy is accessible. The Pd(0) olefin complex **7** (respectively **8**) is 4.0 kcal mol⁻¹ (respectively 4.2 kcal mol⁻¹) less stable than infinitely separated η^3 -allyl and triflate. This energy difference is large enough to prevent direct NMR observation of its equilibrium population at room temperature. Moreover, two ion pairs, **9** (respectively **10**), were optimized (Figure 5) and correspond to an η^3 -allyl interacting with one oxygen atom of the triflate at an energy with respect to separated ions of –6.5 kcal mol⁻¹ (**9**) and –7.5 kcal mol⁻¹ (**10**), respectively. Complexes **9** and **10** are thus ca. 10 kcal mol⁻¹ more stable than complexes **7** and **8**. This result clearly shows that an η^3 -allyl interacting with the counteranion is a much more stable situation than formation of a C–O bond between the allyl and the triflate. The correctness of this thermodynamic conclusion is clear: reaction of Pd(0) sources with allyl triflate is a standard synthesis of cationic Pd(II) allyl complexes.^{21,22}

All of the above calculations have been on singlet states. With regard to the biradical structure mentioned in the Introduction,²³

(21) Tsuji, J. *Transition Metal Reagents and Catalysts*; John Wiley: New York, 2000.

(22) Kurosawa, H.; Yamoto, A. *Fundamentals of Molecular Catalysis*; Elsevier: Amsterdam, 2003; Chapter 3.

(23) The reported ¹H, ¹³C, and ³¹P NMR data indicate the absence of radical character in solution.

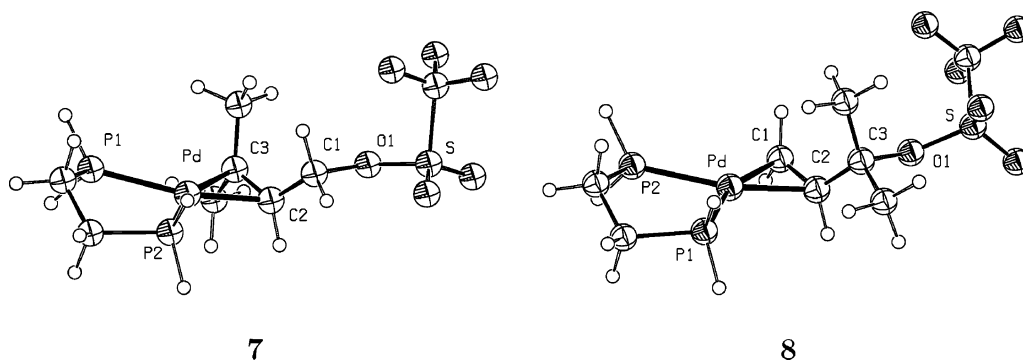


Figure 4. Optimized geometry (B3PW91/CPCM) for the Pd(0) olefin complexes **7** and **8** resulting from C–O bond formation with triflate. For **7**, Pd–C1 = 3.006 Å, Pd–C2 = 2.136 Å, Pd–C3 = 2.153 Å, C2–C3 = 1.422 Å, and C1–O1 = 1.516 Å. For **8**, Pd–C3 = 3.110 Å, Pd–C1 = 2.109 Å, Pd–C2 = 2.144 Å, C1–C2 = 1.415 Å, and C3–O1 = 1.559 Å.

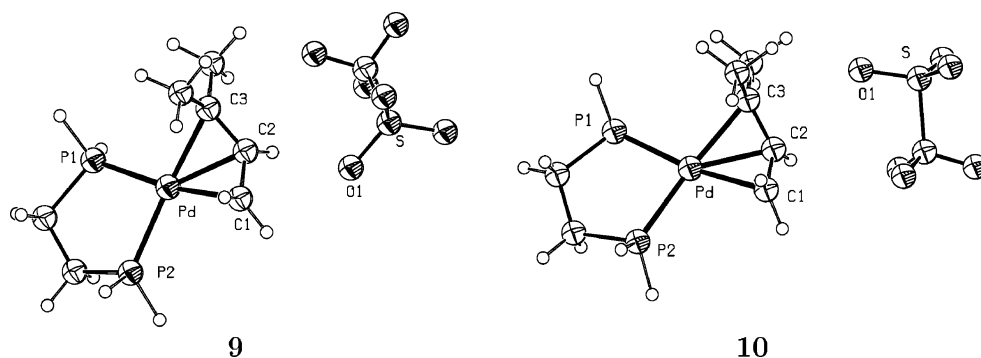


Figure 5. Optimized geometry (B3PW91/CPCM) for the ion pairs **9** and **10** between the η^3 -allyl and the triflate. For **9**, Pd–C1 = 2.164 Å, Pd–C2 = 2.163 Å, Pd–C3 = 2.248 Å, and C1–O1 = 3.098 Å. For **10**, Pd–C3 = 2.226 Å, Pd–C1 = 2.158 Å, Pd–C2 = 2.168 Å, and C3–O1 = 3.069 Å.

geometry optimization of a triplet state from a geometry with a dangling CH₂ group (Pd···C = 2.90 Å) led to an olefin complex (not shown) with C1 and C2 coordinated to Pd (Pd–C1 = 2.28 Å, Pd–C2 = 2.38 Å, C1 = C2 perpendicular to the P–Pd–P plane) and a dangling CMe₂ group (Pd–C3 = 3.0 Å) with an energy 37.5 kcal mol^{−1} above that of **1**. This optimized triplet-state geometry has structure **A**. However, such a pendant radical, and thus Pd(I), has an energy whose mole fraction population is far below the detection limits of the EXAFS experiment.

Reevaluation of the EXAFS Fitting Procedure. The reported EXAFS fitting relied on a new procedure in which each shell is refined iteratively,¹³ in contrast to the more common approach of refining all shells simultaneously. One attraction of the iterative approach, or of the related difference-fit approach, is that it decreases the number of simultaneously variable parameters in each fit. This is important since the data in ref 1 contain approximately 20–22 independent parameters and were modeled with 16 variables. One weakness of iterative or difference refinements is that they are potentially sensitive to false minima, since small errors in the parameters for the dominant scatterer can result in misleading fits for the other shells. This is illustrated by Figure 6, which shows the fit results for a synthetic data set²⁴ of the expected EXAFS for two P at 2.30 Å and three C at 2.20 Å. Global refinements returned the starting parameters (as required, since there was no noise in the data used for this simulation). However, when the Pd–P and Pd–C shells were refined iteratively, two different solutions were found, depending on the choice of starting parameters.

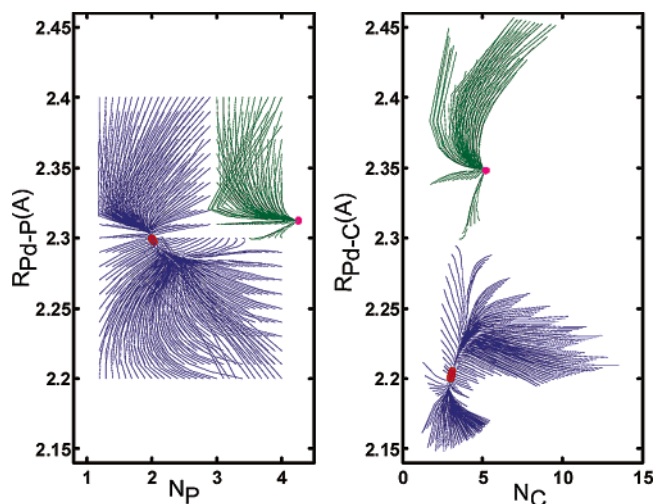


Figure 6. Trajectories showing the iterative refinement of Pd–P parameters (left panel) and Pd–C parameters (right panel) for a synthetic data set (two P at 2.30 Å and three C at 2.20 Å). Initial guesses were made for N_P (between 1 and 4) and for R_{Pd-P} (between 2.2 and 2.4 Å). For each of these, the Pd–C parameters were refined (right panel). Continued iterative refinement of the P and C shells gave a set of trajectories that eventually converged on one of two solutions (marked in red). Trajectories are colored blue or green, depending on the solution to which they converge.

This is illustrated (Figure 6) for different initial guesses of R_{Pd-P} (the Pd–P distance) and N_P (the number of phosphorus centers); similar results are found for other sets of starting parameters. The refinement trajectories from any of the starting parameters shown in blue refine to the actual values which were used to create the EXAFS “data”. The trajectories from the starting parameters shown in green yield a false minimum, in which both N_P and R_{Pd-C} are distinctly too large. In Figure 6, the

(24) The observed EXAFS scattering data were not presented in the paper or Supporting Information of ref 1.

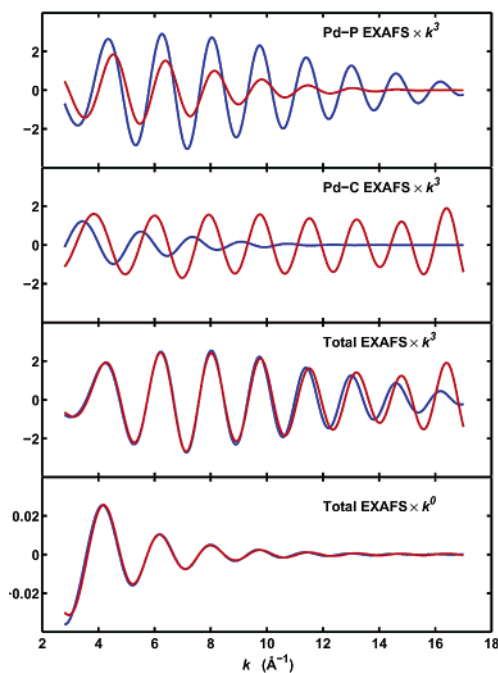


Figure 7. Calculated EXAFS using EXAFS parameters reported for (dppe)Pd[H₂CC(H)CMe₂]⁺. Blue = solid; red = solution. Although these parameters give Pd–P EXAFS (top panel) and Pd–C EXAFS (second panel) that are very different between solid and solution, the total EXAFS (bottom two panels) is identical over most of the k range, differing only at high k , where noise is most serious in any experimental data. k^3 weighting (top three panels) is standard in many EXAFS analyses; both k^3 and k^0 weighting (bottom panel) were used for the fits in ref 1.

Debye–Waller disorder parameter, σ^2 , was fixed at 0.003 Å² to simplify the fits, and the threshold energy, E_0 , was held constant. Relaxation of either of these restrictions leads to more complex fit surfaces, often with more minima. In ref 1, E_0 was allowed to vary, not only between solution state and solid state but also independently for each shell of scatterers. In other studies,¹⁶ treating E_0 as a freely variable parameter has been shown to lead to erroneous conclusions.

The multiple minima in Figure 6 are due to the fact that Pd–P and Pd–C EXAFS oscillations are nearly out of phase. Consequently, small changes in, for example, the Pd–C coordination number can easily be compensated by changes in the Pd–P coordination number and bond length. The fits become even more underdetermined if E_0 and σ^2 are also refined. This compensation is illustrated in Figure 7, which shows the calculated EXAFS using the structural parameters that were reported from the EXAFS analyses of (dppe)Pd[H₂CC(H)CMe₂]⁺. In ref 1, the fits gave a 3-fold increase in σ_{P}^2 and a 15-fold decrease in σ_{C}^2 on going from solid to solution. The former causes a significant decrease in the amplitude of the Pd–P EXAFS (Figure 7, top). This is almost perfectly compensated by the increase in the Pd–C EXAFS amplitude that results from the much smaller σ_{C}^2 and the slightly smaller Pd–C coordination number ($N_{\text{C}}^{\text{(allyl)}}$) that were reported for the solution-phase EXAFS (Figure 7, middle). As noted in the Introduction, the decrease in $N_{\text{C}}^{\text{(allyl)}}$ is responsible for the conclusion which comprises the title of the present paper.

Discussion

Arguing purely from the experimental data, an η^2 -allyl adduct **A** should have very different ¹³C and ¹H NMR parameters from

an η^3 -adduct, displaying either parameters for a carbonium ion or the large range of chemical shifts and broad lines of a paramagnetic species. In addition, it is unclear why this structural change in solution would not also happen for the larger bite angle chelate DPEphos, yet the published solution EXAFS data for this larger chelate show no features for such a rearrangement.

Reference 1 shows that the EXAFS can be modeled by a novel Pd–allyl structure (**A**). However, these fits were performed using a method that has the potential (Figure 6) to give false minima. The authors of ref 1 made use of variable k -weighting and R -space fitting in order to minimize the sensitivity of the method to multiple minima. The minimum corresponding to structure **A** is slightly better than that corresponding to the solid-state structure and clearly represents one possible interpretation of the EXAFS. However, given that there are only subtle differences between the solid- and solution-phase data (Figure 7) and that structure **A** is not supported by theoretical calculations, it is appropriate to ask whether structure **A** is a *reasonable* minimum. Several aspects of the fits in ref 1 are problematic in their own right, independent of any concerns over possible multiple minima. On going from solid to solution, there is a 7 eV decrease in the ΔE_0 value for the Pd–P shell and a 9 eV increase in the ΔE_0 for the 3 Å Pd–C shell. These unusually large changes in E_0 are only seen for the dppe complex and not for the DPEphos complex. The parameter E_0 is used to adjust theoretical calculations to the energy scale of the experimental data and has been found to vary slightly (a few electronvolts) when the metal oxidation state changes. In principle, E_0 should be identical for each scatterer. However, some authors have found it useful to allow each scatterer to have a different E_0 , and this may be justified by the need to correct for small errors in the theoretical EXAFS parameters. What is unusual, and difficult to justify theoretically, is the observation that E_0 varies dramatically between solid and solution for the dppe complex. Much of the ability to distinguish between P and C scattering in EXAFS relies on a phase difference between P and C scattering; when E_0 is allowed to vary, this phase information is lost. It is especially troubling that the unusual variation in E_0 is seen only for the putative new structure **A**.

Even more surprising than the large changes in E_0 are the unexpectedly large changes in the Debye–Waller factors, σ^2 , for the dppe complex on going from solid to solution (there are almost no changes in σ^2 for the DPEphos complex on dissolution). The Debye–Waller factor contains contributions from both static and dynamic disorder: $\sigma^2 = \sigma_{\text{static}}^2 + \sigma_{\text{dynamic}}^2$. As shown in Figure 7 (top), there is a dramatic increase in σ_{P}^2 for the dppe complex in solution. Since $\sigma_{\text{P,dynamic}}^2$ is related to $\nu_{\text{Pd–P}}$, $\sigma_{\text{P,dynamic}}^2$ should depend on $R_{\text{Pd–P}}$. Since $R_{\text{Pd–P}}$ is the same for the solid and the solution, $\sigma_{\text{P,dynamic}}^2$ should be unchanged, at least to a first approximation, meaning that the increase in σ_{P}^2 must result from an increase in $\sigma_{\text{P,static}}^2$. In order for $\sigma_{\text{P,static}}^2$ to increase by 0.007 Å², the two Pd–P distances would have to differ by approximately 0.12 Å. There is no chemical reason for such variation, and this variation is not seen in the calculated (DFT) structure resembling **A**. The 0.014 Å² decrease in σ_{C}^2 (Figure 7, second panel) is equally surprising. On the basis of the reported Pd–C distances (2.174, 2.184, and 2.253 Å), $\sigma_{\text{C,static}}^2$ should be only 0.002 Å². In order for there to be a 0.014

\AA^2 decrease in σ_C^2 , there would have to be a large decrease in thermal motion for the solution-phase sample.

Taken together, the variations in E_0 and in σ^2 suggest strongly that the apparent change in structure when the dppe complex is dissolved in THF is the result of a false minimum in the EXAFS refinement. Further support for this conclusion comes from the fact that the coordination number and the Debye–Waller factor are highly correlated; a decrease in the Debye–Waller factor can be approximately compensated by a decrease in coordination number. It is therefore noteworthy that σ_C^2 is reported to decrease when the dppe complex is dissolved THF. If this is a false minimum, it would have to be accompanied by a corresponding decrease in the apparent Pd–C coordination number. This is precisely what is reported in the EXAFS fits that were the basis for the initial claim of an altered structure in solution.¹

This suggestion that the EXAFS results represent a false minimum is strengthened by the observation that DFT calculations do not support the existence of a singlet-state structure, **A**, as an energetic minimum and by the observation that the solution NMR spectra of ³¹P, ¹³C, and ¹H all show quite normal spectroscopic parameters indicative of an η^3 -allyl complex. In structure **7**, the CH₂ bonded to the triflate is around 3 Å from Pd, which is the distance suggested by the EXAFS measurements. However Pd(0)/olefin structures **7** and **8** are calculated to be of the same energy. One should therefore have observed *two* structures of type **A**, one for uncoordinated CH₂ and one for uncoordinated CMe₂, which is not the case. Likewise, these structures should also have been observed with a diphosphine other than dppe since the triflate anion interacts with the allyl carbon far from the diphosphine ligand. This is also not the case. In other words, the EXAFS fitting with a unique structure among a group of structures which *must* be very close in energy (the calculated *relative* energies of similar systems are highly accurate) also speaks against structure **A**.

The NMR, in particular, could be informative on the possibility of interactions between the cation and the triflate anion.^{25,26} Final proof of whether the structures in solution and in solid are different might be accomplished by a multinuclear *solid-state* NMR study and comparison of those chemical shifts to the published solution values. In addition, the EXAFS data, interpreted as evidence for an unprecedented structural rearrangement on going from solid state to solution, may warrant further study.

Experimental Section

Computational Details. All calculations were performed with the Gaussian 98 set of programs²⁷ within the framework of hybrid DFT (B3PW91)^{28,29} on the model system (dhpe)Pd(H₂CCHCMe₂)⁺. The

ONIOM calculations³⁰ on the model system (dppe)Pd(H₂CCHCMe₂)⁺ were performed with the QM part corresponding to (dhpe)Pd(H₂CCHCMe₂)⁺ treated at the UFF level.³¹ The palladium atom was represented by the relativistic effective core potential (RECP) from the Stuttgart group (18 valence electrons) and its associated (8s7p5d)/(6s5p3d) basis set,³² augmented by an f polarization function ($\alpha = 1.472$).³³ The sulfur and phosphorus atoms were represented by RECP from the Stuttgart group and the associated basis set,³⁴ augmented by a d polarization function.³⁵ A 6-31G(d,p) basis set³⁶ was used for all the remaining atoms of the complex, the Me₂O molecule, and the CF₃SO₃[−] triflate anion. Full optimizations of geometry without any constraint were performed, followed by analytical computation of the Hessian matrix to confirm the nature of the located extrema as minima on the potential energy surface. Optimizations in THF solvent of (dhpe)Pd(H₂CCHCMe₂)⁺ and various adducts with triflate were performed at the B3PW91 level within the CPCM model.^{37–39}

EXAFS Modeling. Phase and amplitude functions of Pd–C and Pd–C EXAFS scattering were calculated using FEFF 7.02.⁴⁰ The synthetic EXAFS data were created using a shell of three carbon atoms at $R_{\text{Pd-C}} = 2.20 \text{ \AA}$ with $\sigma_{\text{Pd-C}}^2 = 0.003 \text{ \AA}^2$ and a shell of two phosphorus atoms at $R_{\text{Pd-P}} = 2.30 \text{ \AA}$ with $\sigma_{\text{Pd-P}}^2 = 0.003 \text{ \AA}^2$. Simulations were done over $k = 2.8\text{--}17.0 \text{ \AA}^{-1}$. The search for local minima in the iterative refinements was done for k^3 -weighted k -space data, using MATLAB Optimization Toolbox v2.2. The nonlinear optimizations were performed in series, optimizing the distance and coordination number for one shell while all other variables were kept fixed.

Acknowledgment. This work was supported in part by the NIH (GM-38047 to J.P.H.) and the NSF (to K.G.C.). We are grateful to Piet W. N. M. van Leeuwen for constructive criticisms of the arguments and on the manuscript.

JA049091G

- (27) Frisch, M. J.; Trucks, G. W.; Schlegel, H. B.; Scuseria, G. E.; Robb, M. A.; Cheeseman, J. R.; Zakrzewski, V. G.; Montgomery, J. J. A.; Stratmann, R. E.; Burant, J. C.; Dapprich, S.; Millam, J. M.; Daniels, A. D.; Kudin, K. N.; Strain, M. C.; Farkas, O.; Tomasi, J.; Barone, V.; Cossi, M.; Cammi, R.; Mennucci, B.; Pomelli, C.; Adamo, C.; Clifford, S.; Ochterski, J.; Petersson, G. A.; Ayala, P. Y.; Cui, Q.; Morokuma, K.; Malick, D. K.; Rabuck, A. D.; Raghavachari, K.; Foresman, J. B.; Cioslowski, J.; Ortiz, J. V.; Baboul, A. G.; Stefanov, B. B.; Liu, G.; Liashenko, A.; Piskorz, P.; Komaromi, I.; Gomperts, R.; Martin, R. L.; Fox, D. J.; Keith, T.; Al-Laham, M. A.; Peng, C. Y.; Nanayakkara, A.; Gonzalez, C.; Challacombe, M.; Gill, P. M. W.; Johnson, B.; Chen, W.; Wong, M. W.; Andres, J. L.; Head-Gordon, M.; Replogle, E. S.; Pople, J. A. *Gaussian 98*, revision A.11; Gaussian, Inc.: Pittsburgh, PA, 1998.
- (28) Becke, A. D. *J. Chem. Phys.* **1993**, *98*, 5648.
- (29) Perdew, J. P.; Wang, Y. *Phys. Rev. B* **1992**, *82*, 284.
- (30) Svensson, M.; Humbel, S.; Froese, R. D. J.; Matsubara, T.; Sieber, S.; Morokuma, K. *J. Phys. Chem.* **1996**, *100*, 19357.
- (31) Rappé, A. K.; Casewitt, C. J.; Colwell, K. S.; Goddard, W. A.; Skiff, W. M. *J. Am. Chem. Soc.* **1992**, *114*, 10024.
- (32) Andrae, D.; Häussermann, U.; Dolg, M.; Stoll, H.; Preuss, H. *Theor. Chim. Acta* **1990**, *77*, 123.
- (33) Ehlers, A. W.; Böhme, M.; Dapprich, S.; Gobbi, A.; Höllwarth, A.; Jonas, V.; Köhler, K. F.; Stegmann, R.; Veldkamp, A.; Frenking, G. *Chem. Phys. Lett* **1993**, *208*, 111.
- (34) Bergner, A.; Dolg, M.; Küchle, W.; Stoll, H.; Preuss, H. *Mol. Phys.* **1993**, *30*, 1431.
- (35) Höllwarth, A.; Böhme, H.; Dapprich, S.; Ehlers, A. W.; Gobbi, A.; Jonas, V.; Köhler, K. F.; Stegmann, R.; Veldkamp, A.; Frenking, G. *Chem. Phys. Lett.* **1993**, *203*, 237.
- (36) Hariharan, P. C.; Pople, J. A. *Theor. Chim. Acta* **1973**, *28*, 213.
- (37) Miertus, S.; Scrocco, E.; Tomasi, J. *Chem. Phys.* **1981**, *55*, 117.
- (38) Miertus, S.; Tomasi, J. *Chem. Phys.* **1982**, *65*, 239.
- (39) Cossi, M.; Barone, V.; Cammi, R.; Tomasi, J. *Chem. Phys. Lett.* **1996**, *255*, 327.
- (40) Zabinsky, S. I.; Rehr, J. J.; Ankudinov, A.; Albers, R. C.; Eller, M. J. *Phys. Rev. B* **1995**, *52*, 2995.

(25) Macchioni, A. *Eur. J. Inorg. Chem.* **2003**, 195.

(26) Pregosin, P. S.; Martinez-Viviente, E.; Anil Kumar, P. J. *J. Chem. Soc., Dalton Trans.* **2003**, 4007.